Mobilya ve Ahşap Malzeme Araştırmaları Dergisi
Furniture and Wooden Material Research Journal
Research Article - Araştırma Makalesi 2025 - 8(2), 265-280

Determination of dielectric properties in oriental beech (*Fagus orientalis* Lipsky) wood

Beytullah Bozali[1]*

ABSTRACT: Today, the wood of the oriental beech (*Fagus orientalis* Lipsky.) is widely used in various applications, including furniture, musical instruments, carvings, and veneer. In this study, the dielectric properties of oriental beech were investigated at AC signal frequencies of 100 Hz–1 MHz in the voltage range of 0–100 V DC, and the effects of different surface conditions on these properties were investigated. The dielectric, thermal and surface free energy behaviors of control wood (CW) and wood soaked in water for two weeks (SW) were analyzed comprehensively. Basic parameters such as specific heat capacity (C_p), real (ε') and imaginary (ε'') dielectric constants, alternating current electrical conductivity (σ_{ac}), free energy component (G/ω), dielectric loss factor ($\tan\delta$) were evaluated in detail within the scope of experimental measurements. SW samples exhibited approximately 1,000-fold higher (ε'') values and a two-to three-fold increase in ($\tan\delta$) compared to CW samples. Furthermore, (σ_{ac}) increased from ~10^{-9} S/m in CW to ~10^{-4} S/m in SW, indicating a significant increase in ionic conductivity due to the higher moisture content. CV samples maintain their insulation properties by showing consistent dielectric properties across the entire frequency range. All measurements were repeated three times (n=3) and the standard deviation was found to be less than 5%. These results show that whereas dry wood retains consistent dielectric performance with low losses, moisture dramatically increases conductivity and dielectric losses.

Keywords: Oriental beech, Dielectric properties, AC conductivity, Frequency

Doğu kayını (*Fagus orientalis* Lipsky.) odununda dielektrik özelliklerinin belirlenmesi

ÖZ: Günümüzde doğu kayın (*Fagus orientalis* Lipsky.) odunu, mobilya, müzik aletleri, oymacılık ve kaplama malzemesi gibi çeşitli alanlarda yaygın olarak kullanılmaktadır. Bu çalışmada, doğu kayınının 100 Hz–1 MHz AC sinyal frekanslarında ve 0–100 V DC gerilim aralığında dielektrik özellikleri incelenmiş ve farklı yüzey koşullarının bu özellikler üzerindeki etkileri araştırılmıştır. Kontrol grubu ahşap (CW) ve iki hafta suda bekletilmiş ahşap (SW) örneklerinin dielektrik, termal ve serbest yüzey enerjisi davranışları kapsamlı şekilde analiz edilmiştir. Deneysel ölçümler kapsamında, özgül ısı kapasitesi (C_p), gerçek (ε') ve sanal (ε'') dielektrik sabitleri, alternatif akım elektriksel iletkenlik (σ_{ac}), serbest enerji bileşeni (G/ω), dielektrik kayıp faktörü ($\tan\delta$) gibi temel parametreler detaylı olarak değerlendirilmiştir. SW örnekleri CW örneklerine kıyasla yaklaşık 1.000 kat daha yüksek (ε'') değerleri ve ($\tan\delta$)'de iki ila üç kat artış göstermektedir. Ayrıca, (σ_{ac}) CW'de ~10^{-9} S/m'den SW'de ~10^{-4} S/m'ye yükselerek, daha yüksek nem içeriği nedeniyle iyonik iletkenlikte önemli bir artış olduğunu göstermektedir. CV numuneleri tüm frekans aralığında tutarlı dielektrik özellikler göstererek yalıtım özelliklerini korumaktadır. Tüm ölçümlerin üç kez tekrarlanmış (n=3) ve standart sapmanın %5'ten küçük bulunmuştur. Bu sonuçlar, kuru odunun düşük kayıplarla tutarlı dielektrik performansını korurken, nemin iletkenliği ve dielektrik kayıplarını önemli ölçüde artırdığını göstermektedir.

Anahtar kelimeler: Doğu kayını, Dielektrik özellikler, AC iletkenliği, Frekans

Article History: Submitted:23.07.2025, Revised: 31.10.2025, Accepted:03.11.2025, Published:23.11.2025, * beytullahbozali@duzce.edu.tr
[1]Düzce University, Düzce Vocational School, Department of Electricity and Energy, Düzce/Türkiye
To cite: Bozali B., (2025). Determination of dielectric properties in oriental beech (*Fagus orientalis* Lipsky) wood, *Furniture and Wooden Material Research Journal*, 8 (2), 265-280, DOI: 10.33725/mamad.1749262

1 Introduction

The dielectric properties of a non-conducting material describe its interaction with electric fields. The dielectric constant is defined as the rate of increase in capacitance of a material in a capacitor compared to a vacuum and is the primary measure of its energy storage capacity (James, 1975). While electrical techniques such as resistivity measurement are widely used because moisture levels affect structural performance, data correction is necessary due to material properties and temperature effects (Otten et al., 2017). Numerous characteristics of electrical conductivity in wood have been documented, including temperature and moisture, hemicellulose, cellulose and lignin, mechanical structure, etc. (Husein and others, 2014). The literature also reports that it fluctuates, especially with respect to electric field frequency and moisture content (James, 1975).

There are many studies in the literature on oriental beech. Some of these studies investigated the screw retention strength of plywood produced with poplar, beech, and eucalyptus veneers (Bal et al., 2015). The effects of color bleaching and varnishing processes applied to oriental beech on the flame-induced combustion characteristics of the material were investigated in another study in the literature (Yalınkılıç et al., 2020). Some of the other studies in the literature are the experimental and numerical analysis of the bending behavior of particleboard and fiberboard reinforced with plywood (Güntekin and Uysal, 2024) and the effect of light intensity on the burning performance of paints used in wood and wood-based panels (Kara et al., 2024).

There is significant research examining the relationship between dielectric properties and environmental and structural parameters parallel to these materials studies. In liquid crystal systems, both real and imaginary components of dielectric permittivity have been successfully predicted depending on frequency, voltage, and doping ratio (Aksoy et al., 2023). In another study, the dielectric behavior of SBR/NR-based rubber insulator material was investigated experimentally under different voltage and frequency conditions. The change in tanδ value in high voltage and frequency applications was analyzed (Akın and Arıkan, 2020). The dielectric properties of rock and pellet samples prepared from jet samples were investigated in the frequency range of 5 Hz–13 MHz under different moisture contents. The measurements revealed that the dielectric constant varied between 3.2–4.4 for the rock sample and 2.9–3.9 for the pellet sample (El Mamı, 2024). They introduce Chapidif, a software that models and analyzes the dielectric functions of aluminum. They note that comparisons with experimental data, such as reflected electron energy loss, improve the model's accuracy and dielectric characterization capabilities (Vos and Grande, 2025). Bentonite composites containing different proportions of cobalt (1%) and nickel (5%) were prepared and, their dielectric and structural properties were investigated (Bashal et al., 2025). The dielectric properties of the χ_3 Borophene structure were investigated by Monte Carlo simulations and the ferroelectric–paraelectric transition behavior of the material was revealed under the influence of crystal field, temperature and coupling forces (Sabbah et al., 2025). CdTe nanoparticles doped with Ni^{2+} ions were synthesized using a microwave-assisted method and were determined to have a hexagonal crystal structure with dimensions of 23–25 nm. Dielectric measurements revealed that the dielectric constant and loss decreased as the frequency increased in the 10 Hz–10 MHz frequency range (Tiwary et al., 2025). $(Bi_{0.85}La_{0.15})(Fe_{0.5}Ti_{0.5})O_3$ ceramic compound was synthesized by the conventional solid-state reaction method, and the dielectric, impedance and magnetic properties of the material were analyzed comprehensively (Joshi et al., 2025). The dielectric properties of starch were also investigated.

This study is based on the hypothesis that water uptake in oriental beech wood significantly increases ion polarization and charge accumulation at the interface, leading to higher dielectric losses (ε″, tanδ) and higher alternating current conductivity (σ_{ac}) compared to dry wood samples. The study sought to determine how frequency and moisture content affect the storage behavior and dielectric loss of oriental beech wood compared to other hardwood species. The effects of wood on its dielectric response are also thoroughly investigated to close a significant gap in the research. Although there is much dielectric research for different types of wood, there are currently few systematic investigations on oriental beech (*Fagus orientalis* Lipsky.). Its dielectric response (ε′, ε″), AC conductivity, and polarization mechanisms across a broad frequency range (100 Hz to 1 MHz) have not been well studied. This study aims to close this gap, theoretically defining the underlying mechanisms and physically interpreting them by thoroughly analysing the dielectric characteristics of oriental beech samples (CW and SW). We also expect to lay a strong basis for interdisciplinary applications such as thermoelectric converters and hybrid acoustic-dielectric materials by elucidating the energy storage and dissipation mechanisms of wood.

2 Materials and Methods

We have chosen a frequency range of 100 Hz to 1 MHz to capture the most important dielectric relaxation events in wood. Ionic and electronic polarization processes predominate above 100 kHz. These processes have been reported in the literature for a range of wood species and composites (Pentoś et al., 2017; Elloumi et al., 2021; Sahin and Ay, 2004). The range of DC voltages used in this study was between 0 and 100 V and chosen to avoid polarization and conduction and to excite the material sufficiently to maintain sample integrity. Similar mechanisms have been reported in studies of oriental beech and other hardwoods. (Torkaman et al., 2022). All electrophysiological measurements in this study were conducted in a controlled laboratory at 20–24 °C and 60–65% relative humidity. Moreover, the consistency and repeatability of the electrical properties were maintained. All voltage measurements were repeated three times for each sample to ensure repeatability. (n = 3) These results represent the mean values of these three replicates.

2.1 Sample preparation

CW test samples were prepared with dimensions of 500 mm x 70 mm x 15 mm, and SW test samples were prepared with dimensions of 250 mm x 70 mm x 15 mm. CW: The untreated control group's samples. The test samples were kept in a lab setting after being air-dried. (20–24°C, 60–65% RH) SW: Water was collected during the trial, and samples were kept in distilled water for two weeks in this experimental group. Its moisture level is typically between 10% and 12%. (Glass and Zelinka, 2010). The SW samples were submerged in water until the humidity level surpassed 100% for two weeks. The electrodes were affixed to the sample's contact surface to create an electric field perpendicular to the conductors. This arrangement was chosen because it ensures a consistent voltage response and reduces anisotropic variability in the spectrum measurements. The CW and SW groups are oriented in the same way to guarantee comparability. This study does not evaluate other grain orientations, such as longitudinal or tangential. As a result, the radial orientation was regulated and maintained during all measurements. Our selection of a constant orientation is further supported by earlier research that discovered significant anisotropy of dielectric characteristics dependent on grain direction in oriental beech wood and other hardwoods (Sahin and Ay, 2004).

2.2 Electric Field

The electric field is defined as the force acting on a unit positive charge and is a vector quantity. Mathematically, the electric field is expressed in Equation (1).

$$\vec{E} = \frac{\vec{F}}{q} \tag{1}$$

In Equation (1), $\vec{E}$ is the electric field vector (N/C or V/m), $\vec{F}$ is the electric force acting on the load, and q is the test load. The presence of an electric field allows the dipoles to align in the direction of the field and create macroscopic polarization in the material (Tinga and Nelson, 1973; Vaydoğan, 2017). When an electric field ($E_{applied}$) is applied to a dielectric material, the molecular dipoles are reoriented, creating a dipole field (E_{dipole}) in the opposite direction. The rearrangement of charges within the material results in polarization (P), which can lead to a decrease in the net electric field. The polarization Equation is given in Equation (2).

$$P = \varepsilon_0 X_e E \tag{2}$$

In Equation (2), P represents the polarization, ε_0 the permittivity of the gap, X_e the electrical susceptibility, and E the electric field applied to the system.

2.3 The Measurement of dielectric properties

Two opposing surfaces of each test sample were covered with 20 mm-wide self-adhesive copper conductive tape to take measurements in the dielectric spectroscopy (DS) experimental setup. Figure 1A The LCR measuring device probes were attached to 10 mm-long sections of the copper conductive tape, creating a capacitor-like structure within the test samples exposed to alternating electric fields. Figure 1B Synchronization between the test system and the test system was verified using an oscilloscope placed at the connection points. A DC bias voltage of up to 100 V is applied in dielectric spectroscopy experiments. This value is chosen to provide sufficient field strength to activate polarization and conductivity phenomena in the samples, thus preventing dielectric breakdown. The selected bias range also corresponds to the safe operating limits of the LCR measurement system (GW Instek 8105G) and is consistent with similar studies on wood and other polymeric insulation materials (Barsoukov and Macdonald, 2005; Elloumi et al., 2021).

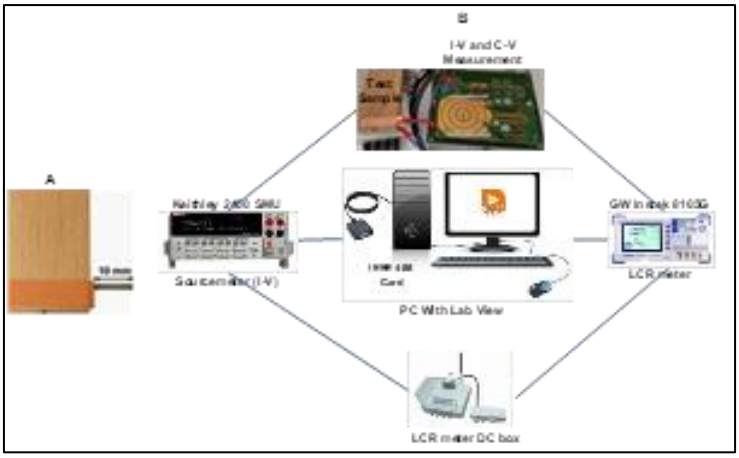

Figure 1. (A) Image of the test sample and (B) DS measurement system used in the study (Demir et al. 2024; İbrahimoğlu et al. 2024; Ramazanoğlu et al. 2025)

Figure 1 Measurement and recording of electrophysical parameters are achieved using a GW Instek 8105G LCR measuring device capable of measuring in the frequency range of 20 Hz to 5 MHz (İbrahimoğlu et al., 2024). The upper frequency limit was chosen as 1 MHz, which corresponds to the reliable operating range of the Instek 8105G GW LCR measuring device used in this study. This limitation was observed in studies where significant relaxation processes were observed below 1 MHz. Similar results were obtained in the literature survey on wood and wood-based composites. (Sahin and Ay, 2004; Pentoś et al., 2017; Elloumi et al., 2021) Beyond this range, electron polarization artefacts and germ forces may affect accurate characterization. Dielectric property measurements were determined using an impedance analysis system equipped with a Keithley 2400 SMU and a GW Instek 8105G LCR measuring device, powered by a computer with an IEEE 488 interface card (Demir et al., 2024; Ramazanoğlu et al., 2025).

The accuracy of the measurement system was validated by us before testing the two test samples. The LCR meter was calibrated with dielectric materials such as air ($\varepsilon' \approx 1.0$), PTFE ($\varepsilon' \approx 2.1$), and glass ($\varepsilon' \approx 4.5–7.0$) (Von Hippel, 1954; Markham, 1964). The determined values agreed with data reported in the literature with a deviation of less than 3%. In addition, the LCR device (GW Instek 8105G) was calibrated at the factory and thoroughly validated according to internal standards (Barsoukov and Macdonald, 2005). System synchronization was tested using an oscilloscope to determine the reliability of the brake response. A low AC signal was applied to the LCR meter to characterize the voltage. Synchronization between the devices was verified with an oscilloscope at the contact points to ensure reliable acquisition of (ε'), (ε''), tanδ, and (σ_{ac}) values over the entire frequency range studied.

The specific heat capacity of the system, Cp (C), is related to the complex dielectric constant.

$$C = C_0 \varepsilon' \tag{3}$$

$$\frac{G}{w} = C_0 \varepsilon'' \tag{4}$$

The capacitance C_0 and conductivity (G/w) values of the composite medium, depending on the frequency, are represented by Equations (1) and (2). In Equations (3) and (4), C is the capacitance, G is the conductivity, $\omega=2\pi f$ is the angular frequency, (ε') is the real dielectric constant (energy storage), (ε'') is the imaginary dielectric constant (energy loss), $C_0=\varepsilon_0.A/d$ is the geometric capacitance. ε_0 is the dielectric permittivity, A is the measured contact area of the composite medium, and d is the thickness of the composite medium (Wei et al., 2016; Demir, 2025).

3 Results and Discussion

In this study, the basic material properties of oriental beech (*Fagus orientalis* Lipsky.) are discussed. Literature indicates that oven-dry density varies between 0.63 and 0.72 g/cm³, and porosity is generally 58-62% (depending on the growing area and anatomical structure). The fiber saturation point (FSP) of beech is generally around 30% moisture content, indicating the transition between bound and free water in the cell walls. These parameters provide important information for understanding the dielectric behavior of wood under different frequency and humidity conditions (Glass and Zelinka, 2010; Sahin and Ay, 2004; Torkaman et al., 2022).

Equations (3)-(4) help understand the variation of properties such as capacity Cp with frequency. The relationship of Cp with frequency is indirectly related to the variation of (ε')

and (ε″) (Kao, 2004). Figure 2a below shows the oriental beech capacitance-frequency variation.

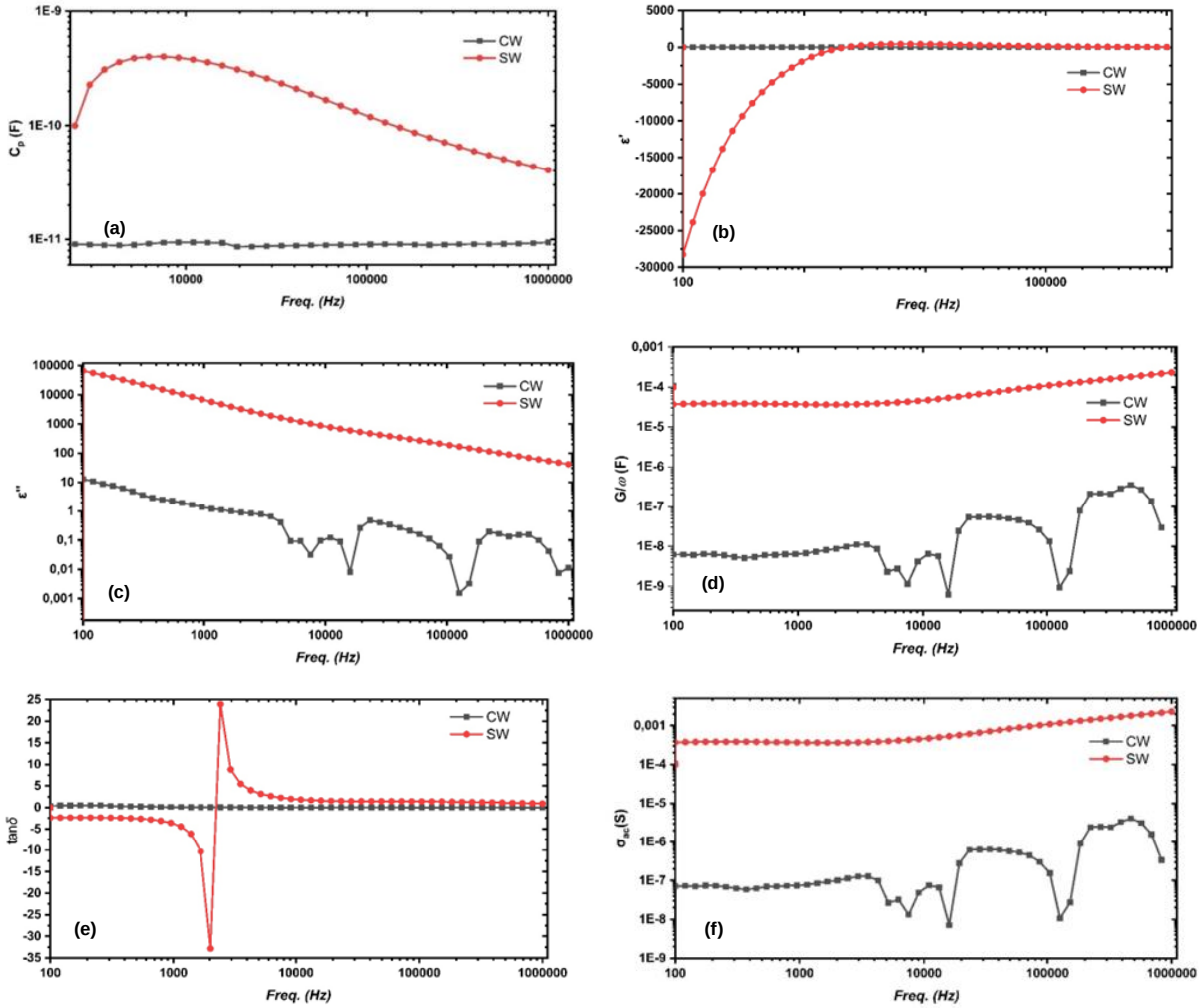

Figure 2. a) Capacitance-frequency variation, b) frequency-dependent behavior of the real dielectric permittivity, c) frequency-dependent behavior of the imaginary permittivity, d) frequency-dependent conductance (G/ω) plot, e) frequency-dependent dielectric loss factor (tanδ) behavior, f) frequency-dependent variation of AC electrical conductivity

The Cp–F graph in Figure 2a shows the change in specific heat capacities (Cp) of two different test samples based on oriental beech, CW and SW, with frequency. While capacitance is a fundamental parameter characterizing the electric charge storage capacity of a material, conductivity is related to the mobility of electrical charge carriers. Ondo-Ndong et al. stated that the decrease in capacitance values observed in materials is inversely proportional to the increase in conductivity values (Ondo-Ndong et al., 2018). Similar trends are observed in dielectric studies on wood composites, where capacitance decreases steadily with increasing frequency, reflecting a weakening of dipolar polarization at high frequencies (Notingher et al., 2003; Porebska et al., 2021).

The experimental CW sample shows extremely low Cp values (~1E-11 F) throughout the whole frequency range. Both dry and wet surfaces are more polarized and have higher dielectric constants (ε′ and ε″). These findings suggest that solute solubility at low and dry temperatures promotes corrosion susceptibility and corrosion product breakdown (Sahin and

Ay, 2004; Pentoś et al., 2017; Glass and Zelinka, 2010). These results may indicate that the absence of moisture significantly limits the energy storage capacity of wood in alternating electric fields. The increased capacitance (Cp) observed in SW samples at frequencies up to 10 kHz can be attributed to the combined effects of ionic and interface polarization (Maxwell-Wagner-Sillars), which lead to charge accumulation at the interfaces between cell wall components and adsorbed water (Sahin and Ay, 2004; Pentoś et al., 2017; Sugimoto et al., 2005). The consistent drop in Cp above 10 kHz indicates that dipoles and interface charges are less able to track an electric field that is changing quickly. This frequency-dependent dielectric dispersion seems to fit Jonscher's description of the universal dielectric response (Jonscher, 1977). Although a detailed curve fitting (e.g., Debye or Cole-Cole modeling) was not performed in this study, the observed trends are consistent with established theoretical frameworks for dielectric relaxation in wood-based materials (Jonscher, 1977; Pentoś et al., 2017).

We can assess the electrical response of a material with both resistive and reactive components using the complex impedance approach, which is frequently employed in dielectric research. The complex impedance Z^* is defined as the sum of the real Z' and imaginary Z'' components. The real (ε') and imaginary (ε'') components of the dielectric constant are derived by Equations (6) – (9) based on the expression for complex impedance ($Z*$) defined in Equation (5) (Gencel et al., 2024; İbrahimoğlu et al., 2024; Demir, 2025).

$$Z^* = Z' + jZ'' \tag{5}$$

Using the impedance spectrum, the complex dielectric constant ε^* is obtained as in Equation (6).

$$\varepsilon^* = \frac{1}{jwZ^*} = \varepsilon' + j\varepsilon'' \tag{6}$$

In Equation (4), ε^* represents the complex permittivity, $\omega=2\pi f$ represents the angular frequency, and C_0 represents the gap capacitance. The real (ε') and imaginary (ε'') components of the complex dielectric constant are calculated as follows using Equation (4).

$$\varepsilon' = \frac{1}{wC_0} \cdot \frac{Z''}{(Z')^2 + (Z'')^2} \tag{7}$$

$$\varepsilon'' = \frac{1}{wC_0} \cdot \frac{Z'}{(Z')^2 + (Z'')^2} \tag{8}$$

$$C_0 = \varepsilon_0 \frac{A}{d} \tag{9}$$

In Equations (7)-(9), C_0 represents the capacitance of free space. In Equation (9), ε_0 represents the dielectric permittivity A of the composite medium and d represents the thickness of the composite material (Demir, 2025).

The ε'–F plot shown in Figure 2b examines the true dielectric constant (ε') values of oriental beech CW and SW test samples in the frequency range of 100 Hz–1 MHz.

The CW test sample (ε') remained positive and constant (in the range of ~1–10) and showed no significant variation with frequency. This indicates a low density within the sample and limited directivity. Its stability, even at high frequencies, demonstrates that the

structure is highly insulating, homogeneous, and has low losses. Therefore, the CW structure can be recommended as a reliable insulating material for applications requiring high-frequency stability.

(ε′) for SW samples exhibit a pronounced dielectric dispersion up to ~10 kHz, followed by stabilization between 30 and 50 kHz. This behavior is consistent with the interface polarization (Maxwell-Wagner-Sillars) at low frequencies and the universal dielectric response reported in dielectric studies of wood and composites (Sahin and Ay, 2004; Jonscher, 1977; Pentoś, et al., 2017; Sugimoto, et al., 2005; Duchow and Gerhardt, 1996).

At very low frequencies, an unusual negative permittivity (~−30,000) is observed in the SW group (Figure 2b). It is due to electrode polarization and charge accumulation at the sample-electrode interface. Similar anomalous dielectric dispersion effects have been reported for wet wood and other high-loss dielectric systems (Sugimoto, et al., 2005; Torgovnikov 1993; Barsoukov and Macdonald 2005). Therefore, negative (ε′) values at low frequencies should be interpreted as an experimental manifestation of interface polarization rather than an intrinsic negative dielectric constant of the material.

SW samples exhibit strong dielectric dispersion at low frequencies, with (ε′) values decreasing sharply up to ~10 kHz and then gradually stabilizing. This behavior is consistent with previous dielectric studies on hardwoods, which reported that the intrinsic permittivity (ε′) decreases with increasing frequency due to interfacial and ionic polarization mechanisms. For instance, Pentoś et al. (2017) discovered that hardwood species like birch and oak had high (ε′) values at low frequencies, which decrease at ~5 kHz. This trend is like our SW results. Similarly, a USDA Forest Products Laboratory report indicates that ε′ in wet wood can vary between ~10^3–10^5 at 1 kHz but stabilizes at ~10–100 at 1 MHz, depending on density and moisture content (Glass and Zelinka, 2010). Compared to these studies, our results show slightly larger scattering magnitudes, which is due to the higher free water content in the SW samples. In contrast, the CW samples exhibit nearly frequency-independent behavior, consistent with drywood systems described in the literature.

The ε″–F plot presented in Figure 2c compares the dielectric losses of the CW and SW materials of two different test samples of oriental beech, using imaginary permittivity (ε″) values measured in the range of 100 Hz–1 MHz. Real permittivity (ε′) represents the energy storage capacity of the system. Virtual permittivity (ε″) reflects the energy loss under the applied alternating electric field, i.e., the fraction converted into heat (Glass and Zelinka, 2010; Pentoś et al., 2017; Sahin and Ay, 2004; Porebska et al., 2021). In dielectric constant calculations based on complex impedance parameters, the (ε″) value is defined by Equation (8).

(ε″) for SW decreases from ~10^5 to ~10^2 in the range 10^2–10^6 Hz. The average slope on a logarithmic scale is approximately -0.7, corresponding to a Jonscher exponent of $s \approx 0.3$. This is consistent with the dielectric response of disordered dielectric systems and shows dispersion determined by interfacial and ionic polarization processes at low frequencies (Jonscher, 1977; Barsoukov and Macdonald, 2005). The high (ε″) values in SW samples, which gradually decline with frequency, show conductivity loss ($\sigma/\omega\varepsilon_0$), which is mostly caused by ion mobility in the adsorbed water phase. The dipolar relaxation of polar groups and bound water is the main cause of the low (ε″) values and slight frequency dependency observed in CW samples. These results confirm that conductivity losses dominate SW, while dipolar relaxation determines the dielectric response in CW SW (Jonscher, 1977; Barsoukov and Macdonald, 2005).

As seen in Figure 2c, the SW model's permittivity (ε″) is much larger than the CW model's and progressively drops with frequency, showing considerable dielectric loss from water polarization and ionic conduction. This outcome is consistent with previous research showing that hardwoods exhibit higher (ε″) values than softwoods due to their lower density and porosity, especially at low frequencies (Pentoś, et al., 2017). For example, oak has a 425% higher absorption coefficient than spruce at approximately 110 kHz, suggesting that pore structure and anatomy influence the dielectric properties. Sahin and Ay (2004) discovered that density and moisture content had a major impact on the dielectric loss of wood, with larger moisture concentrations (ε″) rising in the frequency range. They consistently show that the low and flat values (ε″) of the CW model suggest relatively little ion transfer by dipole relaxation, while the high values (ε″) of the SW model are due to the combined effect of adsorbed water and interface polarization. At very low frequencies, the electrode polarization effect is caused by charge deposition between the electrode and the sample, which can artificially increase the apparent dielectric constant. Furthermore, negative values of (ε′) are observed at high humidity, which is related to the polarization and the dominant conductivity properties of the Maxwell-Wagner interface. There are different studies in literature to explain the dielectric behavior of wood-based materials (Barsoukov and Macdonald, 2005; Jonscher, 1977; Sahin and Ay, 2004).

Several physical processes, including segmental transition, polarization relaxation, and light loss, affect the free energy ratio (G/w) of devices under alternating current. This process is mainly related to the complex dielectric constant (ε″) described by Equation (10).

$$\frac{G}{w} = C_0 \varepsilon'' \tag{10}$$

In Equation (10), G is the conductivity (S), $\omega=2\pi f$ is the angular frequency (rad/s), $C_0=\varepsilon_0 \cdot A/d$ is the geometric capacitance, and (ε″) is the dielectric loss component (Macdonald, 1992; Demir, 2025; Barsoukov and Macdonald, 2005). Equation (11) can be used to conceptualize alternating current (AC) as the conductivity (σ_{ac}) and the loss of conductivity.

$$\sigma_{ac}(w) = \varepsilon_0 w \varepsilon'' \tag{11}$$

Equation (11) determines the electrical conductivity (σ_{ac}(S)) and AC conductivity (S/m) by considering the dielectric loss. Equation (11) uses ε_0 for the gap's dielectric constant (8.854×10^{-12} F/m) and (ε″) for the dielectric loss constant.

$$\sigma_{ac} = A.w^s \tag{12}$$

The frequency-dependent conductance in Equation (12) is determined by an exponential parameter, *s*, and a constant conductance factor, A. The features of a wood-based system's frequency-dependent conductance and conduction mechanism are described by Equation (12). The system's conductance (ε″) changes with frequency. Low conductivity shows the system's ability to store energy and provide insulation, whereas high conductivity suggests that the system tends to lose energy (Macdonald, 1992; Barsoukov and Macdonald, 2005; Demir, 2025). Material's ability to store energy in an alternating field is represented by its real permittivity (ε′), which is mostly caused by electronic, dipolar, and interfacial polarization (Maxwell-Wagner polarization). Equation (11) establishes a direct relationship between the alternating current conductivity (σac) and the imaginary permittivity (ε″), which represents dielectric losses resulting from delayed dipolar orientation and charge carrier hopping. The frequency dependence of (σ_{ac}), generally described by Jonscher's power law Equation (12),

shows hopping and relaxation at low to moderate frequencies, while dipolar and electronic polarization dominate at higher frequencies. The dielectric loss tangent ($\tan\delta = \varepsilon''/\varepsilon'$) represents the ratio of the energy lost to the energy stored. Low tanδ values indicate high dielectric stability, while high tanδ values can correspond to significant losses of relaxation (Jonscher, 1977; Barsoukov and Macdonald, 2005).

The G/ω–F plot shown in Figure 2d shows the frequency-dependent free energy conductance of two different test samples of oriental beech in the frequency range of 100 Hz–1 MHz. G/ω represents the energy loss per unit frequency. High values in SW indicate conduction loss dominated by ion movement, while low values in CW reflect insulation behavior with minimal loss (Barsoukov and Macdonald, 2005; Jonscher, 1977). The predominance of ionic conductivity and ongoing energy loss through water-mediated charge transfer are confirmed by the G/ω values in SW samples, which stay high ($\sim 10^{-4}$ F) and appear to increase progressively over the entire measurement range.

Continuous wave samples have much lower G/ω values ($\sim 10^{-8}$–10^{-7} F) and show minor oscillations above 10 kHz, which are likely due to weak interface polarization and measurement aberrations. Overall, these results demonstrate that while SW samples exhibit substantial conductive loss behavior, continuous wave samples function as insulating systems with minimal energy loss (Barsoukov and Macdonald, 2005; Jonscher, 1977). Similar results were noted by Sugimoto et al. (2005). They asserted that moist wood exhibited higher conduction losses due to Maxwell-Wagner interface polarization, but dry samples behaved more like insulating systems. Furthermore, Pentoś et al. (2017) discovered that hardwoods with higher moisture content consistently displayed increases in dielectric loss characteristics across the whole frequency range, suggesting that absorbed water may contribute to increased ion mobility. These similarities support the hypothesis that SW samples display the normal conduction loss behavior of wet hardwood, even while differences in the fluctuation patterns of CW samples may suggest density- or structure-dependent relaxation anomalies.

The Tanδ-F diagram comparing the dielectric dissipation of SW materials with CW samples in the 100 Hz to 1 MHz frequency range is displayed in Figure 2e. The loss factor (tanδ) is an important parameter since it indicates the energy loss relative to the energy storage capacity of a dielectric material. The CW samples had modest tanδ values and little polarization loss. The SW material, on the other hand, had a decrease in tanδ with frequency, a sign of the relaxation impact of the water. (tanδ) is referred to as the primary parameter that describes a system's dynamic loss. It is crucial to comprehend how power conversion systems and high-frequency equipment operate. Equation (13) calculates the loss factor tanδ from the real (ε') and imaginary (ε'') components of the complex dielectric constant ($\varepsilon^* = \varepsilon' - j\varepsilon''$) (Demir, 2025).

$$\tan\delta = \frac{\varepsilon''}{\varepsilon'} \tag{13}$$

Low tanδ levels have been reported to give the material high dielectric stability and insulating qualities, but high tanδ values are said to result in large energy losses during the dipole steering process (Kao, 2004; Barsoukov and Macdonald, 2005).

The tanδ value of the CW test sample was almost constant (around ~2.5) across frequencies. This suggests steady orientation behavior and good dielectric qualities with minimal energy loss. The low-frequency negative tanδ values (≈ -30) found in SW samples are thought to be artifacts caused by charge accumulation at the interface and electrode

polarization rather than inherent material characteristics. In these circumstances, (ε′) may turn negative, leading to a negative tanδ ratio. Heterogeneous wet dielectrics have also shown a similar anomalous dielectric dispersion, which may be a measurement artifact rather than a real negative loss characteristic (Barsoukov and Macdonald, 2005; Torgovnikov, 1993). Figure 2e also shows a pronounced tanδ peak in SW samples at approximately 1–2 kHz, representing the loss maximum. The corresponding relaxation time ($\tau \approx 1/2\pi f_{max}$) is approximately 10^{-4} s, consistent with interfacial polarization processes (Maxwell-Wagner-Sillars) in water-saturated wood. Conversely, CW samples exhibit low and nearly constant tanδ values over the entire frequency range, suggesting poor dipolar relaxation and strong insulating properties (Jonscher, 1977; Sugimoto, et al., 2005).

At low frequencies (~1 kHz), the SW sample exhibits the characteristic tanδ behavior, which is marked by an abrupt negative peak followed by a significant loss value that stays constant at higher frequencies. This indicates a significant loss of energy due to water-induced ions and interface polarization. However, the CW sample maintained low and consistent tanδ values across the spectrum, indicating good insulation. Similar low-frequency loss peaks are observed for wet wood (Sahin and Ay, 2004; Sugimoto et al., 2005), whereas dry wood tends to show smaller and more uniform tanδ values (Glass and Zelinka, 2010), which is consistent with the results of this study.

Equations (11) and (12) give the AC electrical conductivity (σ_{ac}) equations. AC electrical conductivity (σ_{ac}) is directly related to the ability of a material to conduct free energy lost under an electric field through current. In dielectric systems, (σ_{ac}) reflects the resistive energy component of the system and determines the extent to which free energy is retained or lost. High conductivity indicates that the system tends to lose energy, while low conductivity indicates its insulation and energy storing capacity (Macdonald, 1992; Demir, 2025; Barsoukov and Macdonald, 2005).

Figure 2f (σac–F) plots show the AC electrical conductivity behavior of two different oriental beech test CW and SW samples in the frequency range of 100 Hz to 1 MHz. The conductivity values of the CW test sample versus frequency were quite low (~10^{-7} – 10^{-9} S). However, small sharp spikes were observed in some frequent regions. This indicates that the CW test sample is highly insulated, has limited segmental orientation, and stores energy mostly. The conduction mechanism is weak; the conversion of dipole orientations into free energy is limited. It is suitable for insulation, long-term energy storage, and low-loss capacitive applications. The SW test sample's conductivity value grew somewhat with frequency and stayed high (~10^{-4} S). A smooth logarithmic ascending trend was seen in the curve. This structure implies that the electrical transport mechanism of free ions is activated, and ion mobility is increased by water modification. The SW test sample has poor insulation qualities and is vulnerable to energy losses because of its high (ε") fraction and increased frequency. This is in line with earlier studies that demonstrate how moisture dramatically raises dielectric losses in hardwoods via interfacial polarization and ionic conduction (Sahin and Ay, 2004; Sugimoto et al., 2005; Glass and Zelinka, 2010). The frequency dependence of σ_{ac} in SW samples follows Jonscher's universal power law $\sigma_{ac}(f) = \sigma_0 + Af^s$, where the exponent s reflects the conduction mechanism. According to our observations, σ_{ac} gradually rises with frequency in SW, which is in line with s values for ion-hopping conduction in wet wood systems that have been reported to be between 0.2 and 0.5 (Jonscher, 1977; Sugimoto et al., 2005). Steady-flow samples, on the other hand, show a practically constant σ_{ac} (~10^{-9} S/m), which corresponds to $s \approx 0$, suggesting an insulating characteristic with no frequency dependency.

In the present study, CW samples of oriental beech show low dielectric parameters ($\varepsilon' \approx 10$, $\varepsilon'' \approx 1$, $\tan\delta \approx 0.1$), while SW samples show much higher values ($\varepsilon' \approx 10^3$, $\varepsilon'' \approx 10^4$, $\tan\delta \approx 20$), indicating the presence of strong ionic polarization. Similar trends were observed in hardwoods: oak ($\varepsilon' = 10^2$–10^3, $\tan\delta = 5$–15) and birch ($\varepsilon' \approx 10^2$, $\tan\delta = 4$–10) show higher losses than spruce, a softwood with lower ε' (10–50) and $\tan\delta$ (2–6) values (Pentoś et al., 2017; Sahin and Ay, 2004; Sugimoto et al., 2005). These comparisons verify that the dielectric behavior of moist eastern beech is more pronounced than that of softwoods, although it is still comparable to hardwoods.

The results of the dielectric properties (CW and SW) of oriental beech wood were compared with the values reported in the literature for oriental beech and other hardwood species. The capacitance (Cp), real (ε') and imaginary (ε'') dielectric constants, alternating current electrical conductivity (σ_{ac}), free energy component (G/ω), and dielectric loss factor ($\tan\delta$) are all displayed in Table 1, which summarizes the comparison. The dependability of the results and their applicability to previously published data are confirmed by the fact that the values obtained in this investigation are consistent with the ranges reported for hardwoods under comparable measuring conditions.

Table 1. Comparative dielectric parameters (Cp, ε', ε'', σac, G/ω, $\tan\delta$) of oriental beech wood and literature values reported for other hardwood species.

Parameter	CW	SW	Literature values (hardwoods and moist wood)
Capacitance (Cp)	10^{-11}–10^{-10} F	10^{-9} F	Similar order reported for moist hardwoods (Sugimoto et al., 2005)
ε' (real)	1–10	10^2–10^3	10–10^3 depending on MC and frequency (Pentoś et al., 2017)
ε'' (imag.)	0.1–1	10^2–10^3	Broad range 1–10^3 in moist wood (Sugimoto et al., 2005)
σac (S/m)	10^{-9}	10^{-4}	10^{-8}–10^{-3} (Sahin and Ay, 2004; Pentoś et al., 2017)
G/ω	10^{-8}–10^{-7} F	10^{-4} F	Matches moisture-dependent interfacial polarization (Sugimoto et al., 2005)
$\tan\delta$	0.01–0.1	up to 10^2	Loss tangent strongly moisture dependent (Sahin and Ay, 2004)

4 Conclusion and Suggestions

According to the test results in our study

- Control samples showed continuous specific heat capacity and genuine dielectric permittivity in the low-frequency band when tested for thermal and dielectric stability. This indicates that the molecular structure of wood stuff is stable.
- The dielectric behavior of wood under humid circumstances is more complex than that of SW materials. Unusual phenomena, such as negative permittivity and negative $\tan\delta$, are observed in SW samples at low frequencies. The breakdown of the synchronous dipole orientation brought on by water-induced ion polarization and charge accumulation at the interface can account for these phenomena.
- Because of their high conductivity and potential for energy conversion, SW test samples can be employed in humidity sensors and green energy applications, while CW test samples can be used for insulating properties in high-frequency electronic systems.
- Oriental beaches were the only wood species that were investigated. Additionally, curve-fitting techniques (such as Cole-Cole or Jonscher analysis) were not used to predict aberrant behaviors like negative (ε') and $\tan\delta$ values; this should be considered in subsequent research. Similar techniques can be used to investigate the dielectric characteristics of various wood species. This could aid in the creation of conductive composites and insulation based on biomaterials. Our findings leave two questions unsolved: (i) What effects do longitudinal and tangential anisotropic grain orientations

have on the development of anomalous dielectric behavior? (ii) What effects do high humidity levels have on the change from stable to unstable dielectric responses? Future research addressing these issues will lead to a more thorough comprehension of dielectric mechanisms in wood materials.

Acknowledgement
I would like to thank Prof. Dr. Nevzat Çakicier for his help in providing the wooden material for this study and Assoc. Prof. Dr. Ahmet Demir for providing laboratory facilities for determining the measurements made on the experimental materials.

Author Contribution
Beytullah Bozali: Conceptualization, Determination of methodology, Conducting research, Conducting analyses, Data curation, Resources, Supervision, Validation, Visualization, Drafting the article, Writing, reviewing and editing the article.

Funding Statement
This study was not supported by any organization.

Conflict of Interest Statement
The author declares no conflict of interest.

References

Akın, F., and Arıkan, O., (2020). Harmonik bileşenlerin katı yalıtkan malzemelerin dielektrik performansına etkisi, Elektrik Elektronik ve Biyomedikal Mühendisliği Konferansı, ELECO 2020, Bursa, Türkiye, 1-5.

Aksoy, M., Önsal, G., and Uğurlu, O., (2023). Ni (II)Pc ve CdSeS/ZnS kuantum nokta katkılı sıvı kristal yapıların dielektrik sabitinin makine öğrenmesi algoritmaları ile tahmin edilmesi, *Düzce Üniversitesi Bilim ve Teknoloji Dergisi*, 11(1), 513-523, DOI: 10.29130/dubited.1091499

Bal, B.C., Gündeş, Z., and Akçakaya, E., (2015). Kavak, kayın ve okaliptüs kaplamaları ile üretilen kontrplakların vida tutma direncinin araştırılması, *KSÜ Journal of Engineering Sciences*, 18(2), 77-83.

Barsoukov, E., and Macdonald, J. R., (2005). Impedance Spectroscopy: Theory, Experiment, and Applications, 2nd ed., Hoboken, NJ, USA: Wiley-Interscience.

Bashal, A. H., Khalafalla, M. A. H., and Ibrahim, R. M., (2025). Experimental and semiempirical quantum investigations of the effect of Cobalt addition on the dielectric properties of Nickle-Bentonite composite, *Journal of the Indian Chemical Society*, 102(101696), 1-7, DOI: 10.1016/j.jics.2025.101696

Demir, A., (2025). Multispectral analysis of photosensitive perovskite-E7 liquid crystal composites: Correlating optical response with electrical properties, *Optical Materials*, 162, 1-10, DOI: 10.1016/j.optmat.2025.116878

Demir, A., Musatat, A. B., and Kip, Ş. Z., (2024). Investigation of dielectric anisotropy and electrical modulus-impedance properties of PCBM/E7 composite for organic electronic devices applications, *Celal Bayar Üniversitesi Fen Bilimleri Dergisi*, 21(2), 72-79, DOI: 10.18466/cbayarfbe.1562667

Duchow, K.J., and Gerhardt, R.A., (1996). Dielectric characterization of wood and wood infiltrated with ceramic precursors, *Materials Science & Engineering C-Biomimetic Materials Sensors and Systems,* 4: 125-131.

El Mamı, M. M., (2024). Oltu taşının dielektrik özelliklerinin nem ve frekansa bağlı değişimlerinin incelenmesi, T.C. Selçuk Üniversitesi Fen Bilimleri Enstitüsü, Yüksek Lisans Tezi, Ağustos-2024, Konya.

Elloumi, I., Koubaa, A., Kharrat, W., Bradai, C., and Elloumi, A., (2021). Dielectric properties of wood–polymer composites: Effects of frequency, fiber nature, proportion, and chemical composition, *Journal of Composites Science, 5*(6), 141, DOI: 10.3390/jcs5060141

Gencel, O., Musatat, A. B., Demir, A., Tozluoğlu, A., Tutuş, A., Kıllı, U., Fidan, H., and Kosovalı Cavuş, F., (2024). Transforming industrial byproduct to eco-friendly functional material: Ground-granulated blast furnace slag reinforced paper for renewable energy storage, *Science of the Total Environment*, 954, 1-15, DOI: 10.1016/j.scitotenv.2024.176616

Güntekin, E., and Uysal, M., (2024). Experimental and numerical analysis of the bending behavior of beech (*Fagus orientalis* L.) plywood-reinforced particleboard and fiberboard panels, *Furniture and Wooden Material Research Journal*, 7(1), 26-37, DOI: 10.33725/mamad.1464366

Glass, S. V., and Zelinka, S. L., (2010). *Moisture relations and physical properties of wood*. In *Wood handbook: Wood as an engineering material* (4-1–4-19). USDA Forest Service, Forest Products Laboratory.

Husein, I., Agustina, A., and Khabibi, J., (2014). Electrical properties of Indonesian hardwood case study: *Acacia mangium*, *Swietenia macrophylla* and *Maesopsis eminii*, *Wood Research*, 59(4), 695-704.

İbrahimoğlu, E., Demir, A., Çalışkan, F., and Tatlı, Z., (2024). The dielectric characteristics of spray deposited α-Si_3N_4:ZnO thin films: The nitride effect on frequency-dependent capacitance and conductance profiles, *Solid State Sciences*, 158, 1-10, DOI: 10.1016/j.solidstatesciences.2024.107754

James, W. L., (1975). Dielectric properties of wood and hardboard: Variation with temperature, frequency, Moisture Content, and Grain Orientation Department of Agriculture, Forest Service, Forest Products Laboratory.

Joshi, S., Shukla, A., Kumar, N., and Choudhary, R. N. P., (2025). Investigating the impact of La and Ti co-doping on the structural, morphological, dielectric, electrical, and magnetic properties of bismuth ferrite, *Journal of Alloys and Compounds*, 1026(180383), 1-11, DOI: 10.1016/j.jallcom.2025.180383

Jonscher, A. K., (1977). The ‘universal’ dielectric response. *Nature*, 267, 673–679.

Kao, K.C., (2004). Dielectric phenomena in solids, With Emphasis on Physical Concepts of Electronic Processes, In 1st ed. Amsterdam, Netherlands: Elsevier Academic Press.

Kara, H., Özder, C., Keskin, H., Atar, M., and Karabal, B. N., (2024). Effect of paints applied to wood and wood-based boards on light intensity in combustion, *Furniture and Wooden Material Research Journal*, 7(2), 172-187, DOI: 10.33725/mamad.1563749

Macdonald, J. R., (1992). Impedance spectroscopy, Annals of Biomedical Engineerin, 20, 289-305.

Markham, T. R., (1964). Dielectric constant and loss data. In *Polymer Handbook* (pp. III-1–III-31). Wiley.

Notingher, P., Notingher, P. V., Niţu, C., and Georgescu, D., (2003). Dielectric properties of wood–polymer composites as a function of frequency and moisture. *Polymer Testing, 22*(5), 555–562.

Ondo-Ndong, R., Essone-Obame, H., Moussambi, Z. H., and Koumba, N., (2018). Capacitive properties of zinc oxide thin films by radiofrequency magnetron sputtering, *Journal of Theoretical and Applied Physics*, 12(4), 309-317, DOI: 10.1007/s40094-018-0309-9

Otten, K. A., Brischke, C., and Meyer, C., (2017). Material moisture content of wood and cement mortars – Electrical resistance-based measurements in the high ohmic range, *Construction and Building Materials*, 153, 640-646, DOI: 10.1016/j.conbuildmat.2017.07.090

Pentoś, K., Łuczycka, D., and Wysoczański, T., (2017). Dielectric properties of selected wood species in Poland. *Wood Research, 62*(5), 727–736

Porebska, R., Matykiewicz, D., Barczewski, M., and Andrzejewski, J., (2021). Dielectric properties of wood fiber reinforced polyethylene composites across frequency. *Journal of Composites Science, 5*(6), 141.

Ramazanoğlu, D., Subaşı, A., Musatat, A. B., Demir, A., Subaşı, S., and Maraşlı, M., (2025). Multifunctional SnO2-@ doped glass fiber-reinforced concrete: Improved microstructure, mechanical, dielectric, and energy storage characteristics, *Construction and Building Materials*, 476(141231), 1-15, DOI: 10.1016/j.conbuildmat.2025.141231

Sabbah, H., Fadil, Z., El Fdil, R., Raorane, C. J., Rosaiah, P., AlSayyari, A. A., Fattah, A. A., and Mahmoud, K. H., (2025). Investigating dielectric properties and hysteresis cycles in X3 Borophene: A Monte Carlo study, *Solid State Communications*, 400(115913), 1-8, DOI: 10.1016/j.ssc.2025.115913

Sahin, H., and Ay, N., (2004). Dielectric properties of hardwood species at microwave frequencies, *Journal of Wood Science*, *50*(5), 375–380, DOI: 10.1007/s10086-003-0575-1

Sugimoto, H., Takazawa, R., and Norimoto, M., (2005). Dielectric relaxation due to heterogeneous structure in moist Wood, *The Japan Wood Research Society*, 51, 549-553, DOI: 10.1007/s10086-004-0688-1

Tinga, W., and Nelson, S., (1973). Dielectric properties of materials for microwave processing-tabulated, *Journal of Microwave Power*, 8(1), 23-65, DOI: 10.1080/00222739.1973.11689017

Tiwary, K. P., Mishra, R. K., Nikhil, K., Choubey, S. K., Kumar, S., and Sharma, K., (2025). Investigation of structural, morphological, optical and dielectric properties of Ni^{2}+ modified CdTe nanoparticles, *Physica B: Condensed Matter*, 712(417311), 1-10, DOI: 10.1016/j.physb.2025.417311

Torkaman, J., Aghajankordi, M., and Rangavar, H., (2022). Modification of the beech (*Fagus orientalis*) wood properties via electricity. *Iranian Journal of Wood and Paper Industries, 13*(1), 27–35

Torgovnikov, G. I., (1993). *Dielectric Properties of Wood and Wood-Based Materials*. Springer, DOI: 10.1007/978-3-642-77453-9

Vaydoğan, K. G., (2017). *Isıl işlem görmüş bazı ağaç malzemelerin farklı rutubet şartlarındaki ısı iletkenlik ve dielektrik özelliklerinin belirlenmesi*, Karabük Üniversitesi, Fen Bilimleri Enstitüsü Orman Endüstri Mühendisliği, Yüksel Lisans Tezi, Karabük.

Vos, M., and Grande, P. L., (2025). Dielectric functions, their properties and their relation to observables: Investigations using the Chapidif program for the case of aluminum, *Computer Physics Communications*, 314(109657), 1-20, DOI: 10.1016/j.cpc.2025.109657

Von Hippel, A. R., (1954). Dielectric Materials and Applications. MIT Press.

Wei, L., Liu, Q. X., Zhu, B., Liu, W. J., Ding, S. J., Lu, H. L., Jiang, A., and Zhang, D. W., (2016). Low-cost and high-productivity three dimensional nanocapacitors based on stand-up ZnO nanowires for energy storage, *Nanoscale Research Letters*, 11(213), 1-9, DOI: 10.1186/s11671-016-1429-2

Yalınkılıç, A.C., Aksoy, E., Atar, M., and Keskin, H., (2020). Renk açma ve vernikleme işleminin bazı ağaç malzemelerin alev kaynaklı yanma özelliklerine etkileri, *Mobilya ve Ahşap Malzeme Araştırmaları Dergisi*, 3(2), 61-70, DOI: 10.33725/mamad.750801